



Investigations of compositional separation in Co–Cr–Ta/Cr thin-film recording media

D.J. Rogers ^{a,*}, Y. Maeda ^a, K. Takei ^a, Y. Shen ^b, D.E. Laughlin ^c

^a NTT Basic Research Laboratories, Tokai, Ibaraki 319-11, Japan

^b Read Rite Corporation, 345 Los Coches St, Milpitas, CA 95035, USA

^c Materials Science and Engineering Department, Carnegie Mellon University, Pittsburgh, PA 15213, USA

Received 6 December 1993; in revised form 7 February 1994

Abstract

The compositional distribution in Co–Cr–Ta thin films is investigated as a function of Cr underlayer texture and substrate temperature (T_s) using spin-echo nuclear magnetic resonance and preferential chemical etching. Both the extent and pattern of compositional separation (CS) show no variation with Cr underlayer texture. Elevated T_s is observed to promote both CS and grain boundary Cr enrichment. The magnetic anisotropy fields of Co-enriched components in the films are observed to increase with T_s , explaining the T_s dependence of H_c . Ta addition is observed to control the distribution of Co and Cr, leading to a unique compositional microstructure which may enhance the magnetic and recording properties.

1. Introduction

Co–Cr–Ta films deposited on Cr underlayers have recently received much attention for use as longitudinal magnetic recording media [1,2]. These films are of particular interest because they show large in-plane coercivity (H_c) [1] and low recording noise signals [3].

Two important parameters for achieving good magnetic and recording properties in Co–Cr–Ta films are found to be the substrate temperature (T_s) during deposition of the magnetic film and the crystallographic texture of the Cr underlayer.

The principal role of the T_s for the Co–Cr–Ta film is believed to be the enhancement of compositional inhomogeneity. Indeed, previous studies on Co–Cr–Ta/Cr films deposited at elevated T_s have revealed the occurrence of drastic compositional separation (CS) into distinct Co-enriched and Cr-enriched compositional phases, associated with improvements in the magnetic and recording properties [4].

The principal role of the Cr underlayer is believed to be the promotion of a crystallographic texture in the Co–Cr–Ta film for which the magnetic easy axis lies in, or close to, the plane of the film. It was reported in a previous paper [5], however, that intergranular exchange coupling [6,7], and therefore recording noise, is lower in a film with $\{110\}\text{Cr}/\{1\bar{1}01\}\text{Co–Cr–Ta}$ textures than in a film with $\{200\}\text{Cr}/\{11\bar{2}0\}\text{Co–Cr–Ta}$ textures.

* Corresponding author.

Hence it was proposed that the compositional distribution may also show a dependence on the Cr underlayer texture.

In this study we investigate the compositional distributions in a series of Co–Cr–Ta films as functions of Cr underlayer texture and T_s in order to investigate the possible dependence of CS on the Cr underlayer texture, and to learn more about the effects of T_s and Ta addition on the compositional distribution.

Spin-echo nuclear magnetic resonance (NMR) [8] is employed to measure the extent of CS and preferential chemical etching [9] is employed to reveal the compositional distribution. We also utilize a recent modification of the spin-echo NMR technique [10] to allow measurement of the magnetic anisotropy field for each magnetic component detected in the films.

2. Experiment

Co–Cr–Ta/Cr films were produced by radio-frequency sputter deposition from $\text{Co}_{82.8}\text{Cr}_{14.6}\text{Ta}_{2.6}$ and pure Cr targets, as described elsewhere [5]. We investigated four Co–Cr–Ta/Cr films. In each film the Cr underlayer was 600 Å thick and the Co–Cr–Ta film was 400 Å thick. Co–Cr–Ta films were deposited at initial T_s of either room temperature (low T_s) or 260°C (high T_s) onto both {110} and {200} textured Cr underlayers. Basic physical and magnetic characterization was performed on the films in previous studies [5] (see Table 1).

Spin-echo ^{59}Co NMR studies [8] were conducted on specimens immersed in liquid He (4.2

K) with no external magnetic field. In this technique radio-frequency pulses are applied to the specimen and the echo amplitude is measured as a function of input pulse frequency, with input pulse amplitude fixed at a value which maximises the echo signal. This ‘frequency spectrum’ is then corrected for enhancement and Boltzmann factors through division of the echo amplitude by the square of the input signal frequency (F^2). Using this approach, the spectrum for a pure hcp Co sample exhibits a sharp main peak at approximately 220 MHz. As Cr is introduced the main peak becomes broader and shifts to lower frequency. Hence, by comparing our frequency spectra with those for compositionally homogeneous Co–Cr samples we can estimate the composition of any Co-enriched components present in our films. This technique is valid in the study of Co–Cr–Ta films if we assume that the distribution of Ta atoms affects the spectrum in a similar manner to the distribution of Cr atoms [4].

It has also been demonstrated recently for a Co–Cr specimen [10] that magnetic components with different values of anisotropy field can be discerned using spin-echo NMR. If we measure the echo amplitude as a function of input pulse amplitude, for a fixed input frequency, the input pulse amplitude corresponding to a maximum in echo amplitude is proportional to the anisotropy field of the associated magnetic component in the specimen. If multiple maxima appear in the echo amplitude/input pulse amplitude spectrum we can then isolate distinct magnetic components, measure the relative values of their anisotropy fields and estimate their compositions by collecting the corresponding frequency spectra.

Table 1
Previously reported T_s , crystallographic texture and magnetic properties for all four Co–Cr–Ta/Cr films [5]

| Specimen | A | B | C | D |
|-------------|---------------|---------------|---------------|---------------|
| T_s (°C) | RT/RT | RT/260 | 260/RT | 260/260 |
| Co–Cr–Ta/Cr | | | | |
| Texture | {110̄1}/(110) | {112̄0}/(200) | {110̄1}/(110) | {112̄0}/(200) |
| Co–Cr–Ta/Cr | | | | |
| Delta M | Peak = +0.58 | Peak = +0.68 | Peak = +0.07 | Peak = +0.17 |
| H_c (Oe) | 788 | 796 | 1662 | 1752 |
| (in-plane) | | | | |

Preferential chemical etching of Co was conducted by immersing specimens in dilute aqua regia until a significant decrease in mean Co content was detectable using X-ray microanalysis. Thinned regions of specimen then revealed the original distribution of Co-enriched regions in the films [9]. Since Cr and Ta are both resistant to etching with aqua regia it was not possible to differentiate between the distributions of Cr and Ta. Recent work showing a linear increase in the lattice parameter with Ta content [11], however, suggests that Ta distributes nearly homogeneously in Co–Cr–Ta films. Thus we discuss the observed patterns in terms of the distributions of Co and Cr.

3. Results and discussion

3.1. Spin-echo nuclear magnetic resonance

NMR frequency spectra were acquired for a compositionally homogeneous bulk sample of the target alloy and for all four Co–Cr–Ta films. In order to produce the compositionally homogeneous reference sample, powdered $\text{Co}_{82.8}\text{Cr}_{14.6}\text{Ta}_{2.6}$ was annealed for 2 h at 900°C and then cooled at a rate of 0.2°C/min. Fig. 1 shows the corresponding NMR spectrum, in which we can see a very broad peak centred at a frequency of approximately 50 MHz.

Fig. 2 shows the NMR spectra for the thin film samples. Since a typical area of specimen for NMR study was of the order of 6 cm² we recorded relatively weak echo signals, just resolvable over instrumental noise. From these spectra, however, we can readily see that the Co–Cr–Ta films deposited at 260°C (Figs. 2(c) and (d)) both show relatively sharp main peaks centred at a frequency of approximately 215 MHz. Thus drastic compositional separation (CS) occurred in these films, producing Co-enriched compositional phases with approximately 94 at% Co [8].

The spectra for the Co–Cr–Ta films deposited at low T_s both show broader main peaks centred at a frequency of approximately 200 MHz (Figs. 2(a) and (b)). These correspond to Co-enriched phases with approximately 88 at% Co [8]. Thus

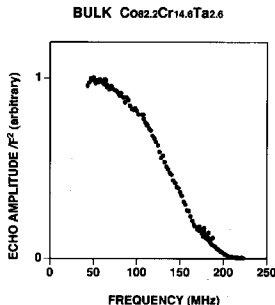


Fig. 1. Spin-echo NMR frequency spectrum for an annealed, powdered, bulk $\text{Co}_{82.8}\text{Cr}_{14.6}\text{Ta}_{2.6}$ sample.

slight CS also occurred in the films deposited at low T_s .

By measuring the echo amplitude as a function of input pulse amplitude we then detected a second echo maximum condition for both the Co–Cr–Ta films deposited at low T_s , Figs. 3(a) and (b) show the corresponding NMR frequency spectra. These spectra both have relatively sharp main peaks centred at a frequency of approximately 210 MHz. This is indicative of strong CS producing Co-enriched phases with around 92 at% Co. Thus there was a second magnetic component in each low- T_s film. From the input pulse amplitude we observed that the magnetic anisotropy field for the second component was similar to that in the films deposited at high T_s , and approximately twice that of the 88 at% Co component.

No second echo maximum condition was detected for the Co–Cr–Ta films deposited at high T_s .

Thus the Co contents and magnetic anisotropy fields of Co-enriched components detected in the Co–Cr–Ta films by NMR were observed to increase with T_s and to be independent of Cr underlayer texture.

3.2. Preferential chemical etching

Fig. 4 shows TEM micrographs of the chemically etched microstructures in the two Co–Cr–Ta films deposited at high T_s . From these images we see that both films have grains of between 30 and 50 nm in diameter, with relatively broad and dark grain boundaries, suggesting the occurrence of strong grain boundary segregation of Cr. Within the grains in both films we can also see a strong etched microstructure which resembles a honeycomb, with dark cores between 5 and 10 nm in

diameter surrounded by a connected network of bright, Co-enriched boundaries.

Fig. 5 shows micrographs of the chemically etched microstructures in the Co–Cr–Ta films deposited at low T_s . A similar honeycomb-like in-grain etched microstructure is observed for both films, with small Cr-enriched cores surrounded by Co-enriched boundaries. There is no evidence of the dark, Cr-enriched, grain boundaries observed in the high- T_s films. Indeed, we can see clearly in Fig. 5(a) that some grain boundaries in the $\{110\}\text{Cr}/\{1\bar{1}01\}\text{Co-Cr-Ta}$ film

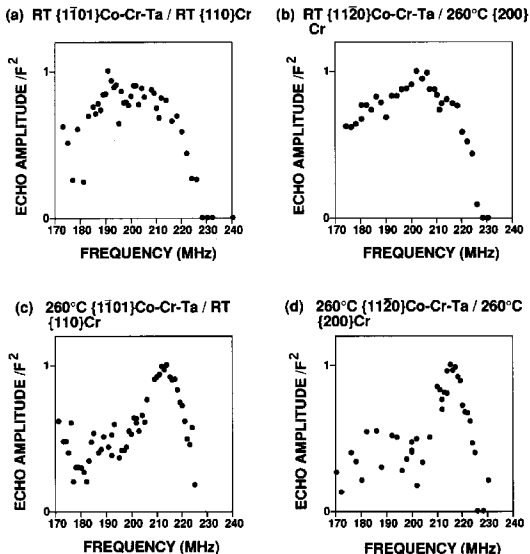


Fig. 2. Spin-echo NMR frequency spectra for all four Co–Cr–Ta/Cr films.

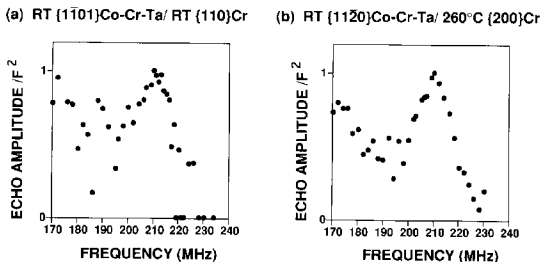


Fig. 3. Spin-echo NMR frequency spectra for the second magnetic component in Co-Cr-Ta films deposited at low T_s .

have many bright dots, which could be due to grain boundary microvoids and/or the occurrence of local Co enrichment.

3.3. Discussion

For Co-Cr-Ta films deposited at both low and high T_s , neither the NMR spectra nor the chemically etched pattern showed any obvious dependence on Cr underlayer texture. It is likely,

therefore, that the observed reduction in ΔM [6,7] for films deposited on $\{110\}$ -textured Cr underlayers is attributable to differences in physical microstructure. Indeed, it has been reported that physical separation between grains in the Cr underlayer is promoted in the kind of low- T_s deposition process employed to produce the $\{110\}$ Cr texture in our films [12]. This would be expected to affect the grain boundaries in the Co-Cr-Ta film. If we reconsider the etched microstructures

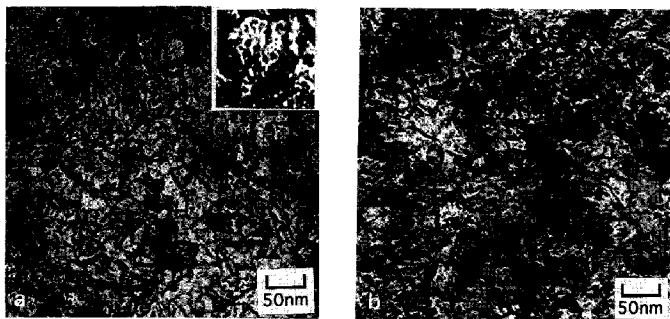


Fig. 4. TEM micrographs of the chemically etched microstructures in the Co-Cr-Ta films deposited at high T_s , with higher magnification inset in (a), showing in-grain structure.

for the Co–Cr–Ta films deposited at elevated T_s (Fig. 4) we can see that the grain boundary Cr enrichment appears more extensive in the film deposited on a {110}-textured Cr underlayer. For the films deposited at low T_s (Fig. 5) only the film deposited on {110} Cr shows a 'dot-like' structure at the grain boundaries. Thus the grain boundaries in Co–Cr–Ta films deposited on {110} Cr appear to be different from the grain boundaries in films deposited on {200} Cr.

Concerning the role of T_s , the NMR spectra for each of the Co–Cr–Ta films deposited at low T_s indicate the presence of two distinct Co-enriched components with different magnetic anisotropy fields. Hence these films appear to be in an intermediate state between an almost compositionally homogeneous film and a film with strong CS. Chemical etching, however, reveals no evidence of Cr segregation to grain boundaries. For films deposited at elevated T_s , on the other hand, we detected drastic CS, producing a single highly Co-enriched component and strong Cr enrichment at the grain boundaries. The occurrence of strong segregation of Cr to the grain boundaries in these films provides experimental evidence in support of the proposal that the reduced delta M for films deposited at elevated T_s corre-

sponded to reduced intergranular exchange coupling [6,7].

Regarding the effect of T_s on other magnetic properties, a detailed NMR study revealed that both the Co contents of Co-enriched components in the films and the strengths of the corresponding anisotropy fields increased with T_s , but did not vary with Cr underlayer texture. This could explain why the coercivity (H_c) was strongly enhanced at elevated T_s but was largely independent of Cr underlayer texture [5].

Regarding the role of Ta addition, it is interesting to consider the unique features of the chemically etched pattern observed in these films. First, the Cr-enriched boundary regions in the films deposited at high T_s were much broader than those observed in films without Ta [9,13]. This did not appear to be linked to diffusion of Cr from the Cr underlayer since X-ray microanalysis revealed a mean film Cr content equivalent to that of the target to within ± 1 at%. Second, the honeycomb-like etched microstructure within the grains in all the films resembled a subgrain structure [12,14] with Co enrichment at the boundaries of Cr-enriched subgrains. This is markedly different from the radially oriented Co- and Cr-enriched 'stripes' of the chrysanthemum

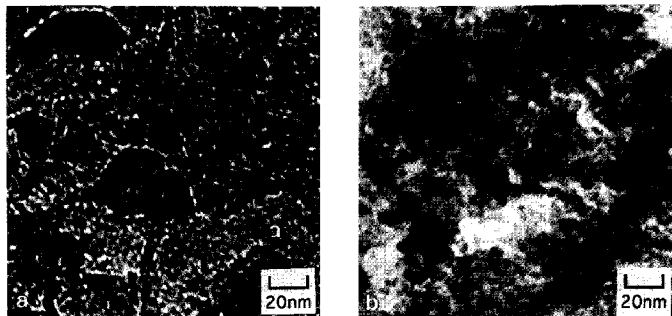


Fig. 5. TEM micrographs of the chemically etched microstructures in the Co–Cr–Ta films deposited at low T_s .

pattern compositional microstructures typically observed in Co–Cr and Co–Cr–Pt/Cr films deposited under similar conditions [9,13].

Thus Ta addition appears to significantly alter the distributions of Co and Cr, leading to a high density of non-, or weakly ferromagnetic sites within each grain and an enhanced reduction in exchange coupling at the grain boundaries for films deposited at elevated T_s . These should be important factors in promoting the low recording noise signal obtained with Co–Cr–Ta media [3].

4. Conclusions

Spin-echo NMR and preferential chemical etching have proven very effective in the study of the compositional distribution in Co–Cr–Ta/Cr thin films.

In this study we observed that the extent and pattern of CS in Co–Cr–Ta films are independent of the crystallographic texture in the Cr underlayer and concluded that the reduction in intergranular exchange coupling for films deposited on a {110}-textured Cr underlayer probably had a microstructural origin related to the grain boundaries.

The Co contents and magnetic anisotropy fields of Co-enriched components detected in the Co–Cr–Ta films by NMR were observed to increase with T_s and to be independent of Cr underlayer texture. This could explain the T_s dependence of H_c .

Finally, it was proposed that Ta addition promoted good magnetic and recording properties

through control of the distributions of Co and Cr, leading to a unique compositional microstructure with a broad band of Cr enrichment at grain boundaries and a fine in-grain distribution of Cr-enriched cores with Co-enriched boundaries.

References

- [1] R.D. Fisher, J.C. Allen and J.L. Pressesky, *IEEE Trans. Magn.* 22 (1986) 352.
- [2] M.R. Khan, S.Y. Lee, S.L. Duan, J.L. Pressesky, N. Heiman, D.E. Speliotis and M.R. Scheinfein, *J. Appl. Phys.* 69 (1991) 4745.
- [3] J.A. Christner, R. Ranjan, R.L. Peterson and J.I. Lee, *J. Appl. Phys.* 63 (1990) 3260.
- [4] Y. Maeda and K. Takei, *IEEE Trans. Magn.* 27 (1991) 4721.
- [5] Y. Shen, D.E. Laughlin and D.N. Lambeth, *IEEE Trans. Magn.* 28 (1992) 3261.
- [6] K. O'Grady, *IEEE Trans. Magn.* 26 (1990) 1570.
- [7] I.A. Beardsley and J.-G. Zhu, *IEEE Trans. Magn.* 27 (1991) 5037.
- [8] K. Takei and Y. Maeda, *Jpn. J. Appl. Phys.* 30 (1991) 1125.
- [9] M. Takahashi and Y. Maeda, *Jpn. J. Appl. Phys.* 29 (1990) 1705.
- [10] K. Takei, D.J. Rogers and Y. Maeda, *Jpn. J. Appl. Phys.* 33 (1994) 1027.
- [11] Y. Deng, D.N. Lambeth and D.E. Laughlin, *IEEE Trans. Magn.* 29 (1993) 3676.
- [12] T.P. Nolan, R. Sinclair, R. Ranjan and T. Yamashita, *IEEE Trans. Magn.* 29 (1993) 292.
- [13] H. Suzuki, N. Goda, S. Nagaïke, Y. Shiroishi, N. Shige and N. Tsumita, *IEEE Trans. Magn.* 27 (1991) 4718.
- [14] T. Yogi and T.A. Nguyen, *IEEE Trans. Magn.* 29 (1993) 307.